Electrochimica Acta 148 (2014) 276–282

Contents lists available at ScienceDirect

Electrochimica Acta

journal homepage: www.elsevier.com/locate/electacta

The electrocatalytic properties of lithium copper composite in the oxygen reduction reaction

M. Farsak [a], E. Telli [b], F. Tezcan [c], F.S. Akgül [c], A. Ongun Yüce [c], G. Kardaş [c,*]

[a] Osmaniye Korkut Ata University, Science and Letters Faculty, Chemistry Department, 80000 Osmaniye, Turkey
[b] Osmaniye Korkut Ata University Engineering Faculty Energy Systems Engineering Department, 80000 Osmaniye, Turkey
[c] Çukurova University, Science and Letters Faculty, Chemistry Department, 01330 Adana, Turkey

ARTICLE INFO

Article history:
Received 28 September 2014
Received in revised form 14 October 2014
Accepted 15 October 2014
Available online 19 October 2014

Keywords:
Oxygen reduction reaction
catalyst
lithium
copper
TEM

ABSTRACT

A new carbon supported lithium-copper cathode catalyst (gel@LiCu) is composed of activated carbon (@) supported gel, $LiNO_3$ and $CuCl_2$ mixture is investigated in the oxygen reduction reaction. The gel@LiCu cathode, which is selected from different configurations of electrodes, is found to have the best material for the cathode. The molar ratio of lithium-copper (1.0:1.5) and the amount of glycine given in terms of grams are determined in order to find the most active material. The catalytic activity of the gel@LiCu electrode is evaluated by cyclic voltammetry, potentiodynamic polarization and electrochemical impedance spectroscopy techniques. The morphology and the phase structure of the gel@LiCu electrode are characterized with scanning electron microscopy (SEM), transmission electron microscopy (TEM) and X-ray diffraction (XRD) spectrometer. The catalyst shows good catalytic activity for oxygen reduction reaction (ORR), as well as oxygen evolution reaction (OER).

1. Introduction

In recent years, batteries have been keenly investigated because of the development of transportable electric vehicles. New technology items run with high-capacity batteries. Lithium air batteries, which use oxygen molecules of the atmosphere, have higher energy than other battery types and they have been studied as promising candidates for high-energy density secondary batteries [1–5]. The rechargeable lithium - ion (Li-ion) batteries have been used for portable electronic appliances such as mobile phones, music players, etc. As the electrical devices have been developed, the energy density of Li-ion batteries has become insufficient [6]. Li-ion batteries have other disadvantages as well. For instance the specific capacitiy of lithium ion batteries are limited by the weight of the anode and cathode materials such as typically graphite (170 mAh g^{-1}) for the anode and metal oxide such as $LiCoO_2$ (130 mAh g^{-1}) for the cathode [7,8]. The cathode materials used for Li-ion batteries are restricted in nature. Therefore, most of the cathode materials are prepared by high-temperature solid-state reactions, which results in consumption of energy and CO_2 emission [9]. What is more, cathodes of conventional lithium-ion batteries are not renewable (or reusable) [10]. It seems that the solution for these challenges requires developing a new concept of the lithium battery. In 1996, Abraham and Jiang first reported the Li-air battery using an organic electrolyte [3]. Lithium air batteries are attracting more and more attention because of their energy and power density.

There are four types of Li-air batteries; aprotic, aqueous, solid state and mixed aqueous/aprotic. We used the aprotic type for our battery tests. The aprotic type consists of four parts; a lithium metal anode, a solid electrolyte interface, an aprotic electrolyte and an air cathode [11]. The battery functions as follows:

$$2Li + O_2 \underset{\text{discharge}}{\overset{\text{charge}}{\rightleftharpoons}} Li_2O_2 \quad (1)$$

when Li_2O_2 is formed at the cathode during discharge, and

$$4Li + O_2 \underset{\text{discharge}}{\overset{\text{charge}}{\rightleftharpoons}} 2Li_2O \quad (2)$$

when Li_2O is formed at the cathode, which has also been reported under certain conditions [12–15].

During the charge process both the above reactions turn vice versa, which plays an important role in the lithium oxide decomposition (mainly lithium peroxide) and the oxidation of peroxide anions (oxygen evolution reaction, OER). These batteries have several restrictions of use in electrical devices, such as slow

* Corresponding author. Tel.: +90 322 338 6084/2593; fax: +90 322 338 6070.
E-mail address: gulfeza@cu.edu.tr (G. Kardaş).

http://dx.doi.org/10.1016/j.electacta.2014.10.066
0013-4686/

kinetics of the ORR and OER during discharge and charge, respectively [16,17]. Recent studies show that the battery performance can be affected by catalysts [18,19].

Porous structures are preferred in the cathode section of lithium air batteries. Carbon materials have been widely studied as cathode materials for Li-air batteries due to their large pore volume, high surface area and electrical conductivity[20–22]. The cathode catalysts are usually carbon black or carbon loaded with a noble metal, which is used to catalyze the air reactions [23]. Pores of carbon materials can act as a path for oxygen access and an electrolyte reservoir, and they can also be holders of the discharge product (Li_2O_2) on space for non-aqueous Li-air batteries [24].

Many studies have been performed to improve OER kinetics and reduce charge overpotential [25–28]. Different types of materials such as carbon-based materials [26,28], noble metals [18,29], metal oxides [30,31] and nitrides [32,33], perovskites [34,35], and pyrochlores [36,37] have been used as catalysts in nonaqueous LiO_2 batteries. Shao-Horn et al. [38] have studied the effects of Pt–Au nanoparticles on the voltage gap between the ORR and OER as a bifunctional catalyst. They have found that Au enhances the ORR and Pt decreases the OER voltages.

Transition metals tender cheaper cost alternative catalysts. Copper is used as the renewable cathode material, because it reduces the oxygen of air and it shows a high capacity in lithium air batteries. The copper nanoparticles play two different roles in the catalyst. First, copper nanoparticles improve the conductivity of the catalysts. Second, the metallic copper can accelerate the ORR at its surface, starting from the copper corrosion in aqueous solution [39,40]. The concept of Li–Cu cathode using in Li-Air battery may provide a new direction for the study of future lithium batteries [9]. $CuSO_4$, CuV_2O_6, CuO-V_2O_5, Cu_6Sn_5, perovskite loaded with copper nanoparticles, Co_3O_4 microspheres loaded with copper and Li-Cu have been used as cathode materials in different studies [9,23,39,41–44]. When lithium ions move into the spinal matrix, the electrocatalytic activity enhances toward the OER [45–47].

The aim of this study is to prepare a lithium-copper cathode catalyst, including activated carbon, which has a high catalytic efficiency when used in lithium air battery cells. Therefore, gel, $LiNO_3$ and $CuCl_2$ were used to build a matrix for bifunctional metals and to improve the ORR and OER performance, respectively.

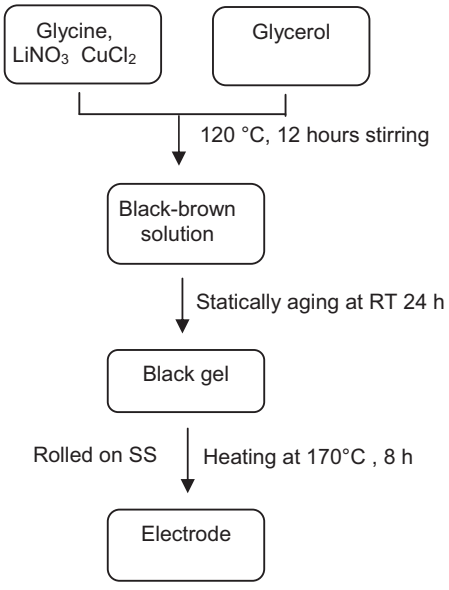

Fig. 1. Scheme for preparation of cathode catalyst.

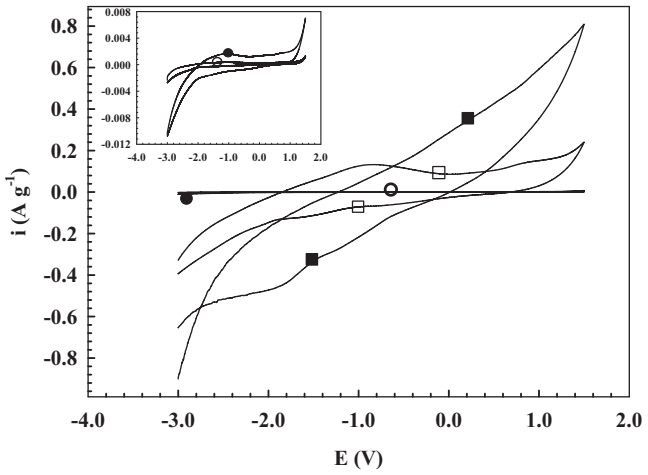

Fig. 2. Cyclic voltammograms of gel (○), gel/Li (●), gel/LiCu(□) and gel@LiCu(■) electrodes at 100 mV s^{-1} scan rate in LED solution.

2. Experimental

All used chemicals, which were purchased from Merck Millipore Co., Ltd. Germany were of analytical or chemical grade purity. The catalysts were prepared by the sol-gel method using glycine, glycerol, $LiNO_3$ and $CuCl_2$. The flow chart of catalyst preparation is shown in Fig. 1. Glycine, glycerol, ammonia, lithium and copper salts were mixed in a pressure resistant Schlenk tube. Then different temperatures and times were applied to obtain a viscous mixture. 12 hours and 120 °C were selected as the most suitable temperature and time. After that the viscous mixture was statically aging for 24 hours at room temperature. Following this process, one part of the gel was rolled and left to paste on a stainless steel plate (SS) at 170 °C for 8 hours in order to make an electrode. Gel was prepared from glycine and glycerol, which were used as the chelating agent and the polymerization precursor, respectively.

The catalysts were characterized by using cyclic voltammetry (CV), potentiodynamic polarization and electrochemical impedance spectroscopy (EIS) techniques. Gamry (interface 1000) model electrochemical analyzer (serial number: 2,009) was used for electrochemical measurements under computer control. A double-wall one-compartment cell with three electrode configuration was

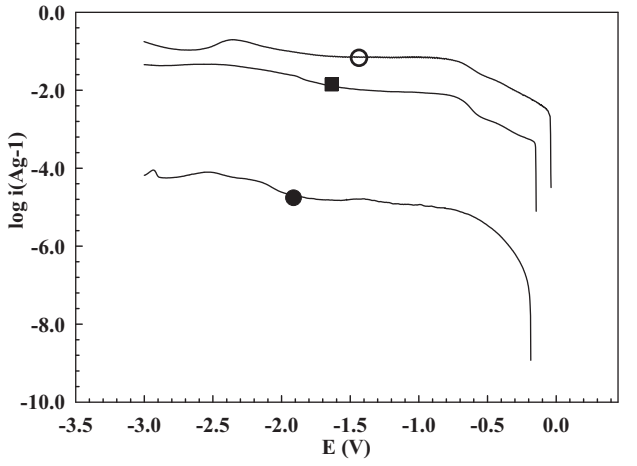

Fig. 3. Current-potantial curves of SS (●), gel@Li (□) and gel@LiCu (○) electrodes under oxygen atmosphere at 1 mV s^{-1} scan rate in LED solution.

used. Platinum electrodes were used as both counter and reference electrodes with 1.188 V (vs. SHE) reference potential. All the experiments were repeated at least three times. The electrolyte which was a mixture of lithium perchlorate, ethylene carbonate and dimethyl carbonate by a weight ratio of 45:45:10 respectively was named the LED solution. EIS measurements were made in a frequency interval of 10^5 Hz and 0.01 Hz and by applying 0.005 V amplitude to the system. Surface images were taken with scanning electron microscopy (SEM, Coxem CX-200) and Transmission Electron Microscopy (TEM, Jem Jeol 2100 F 200 kV HRTEM). N_2 adsorption isotherms of the catalysts used in the investigation were obtained at 77 K using analyzers of the surface area and porosity (Gemini VII 2390). Pore size, pore volume and surface area were calculated according to the Brunauer-Emmett-Teller (BET) method. Gel@LiCu, lithium metal and whatman GF/D were used as cathode, anode and separator, respectively, measuring oxygen

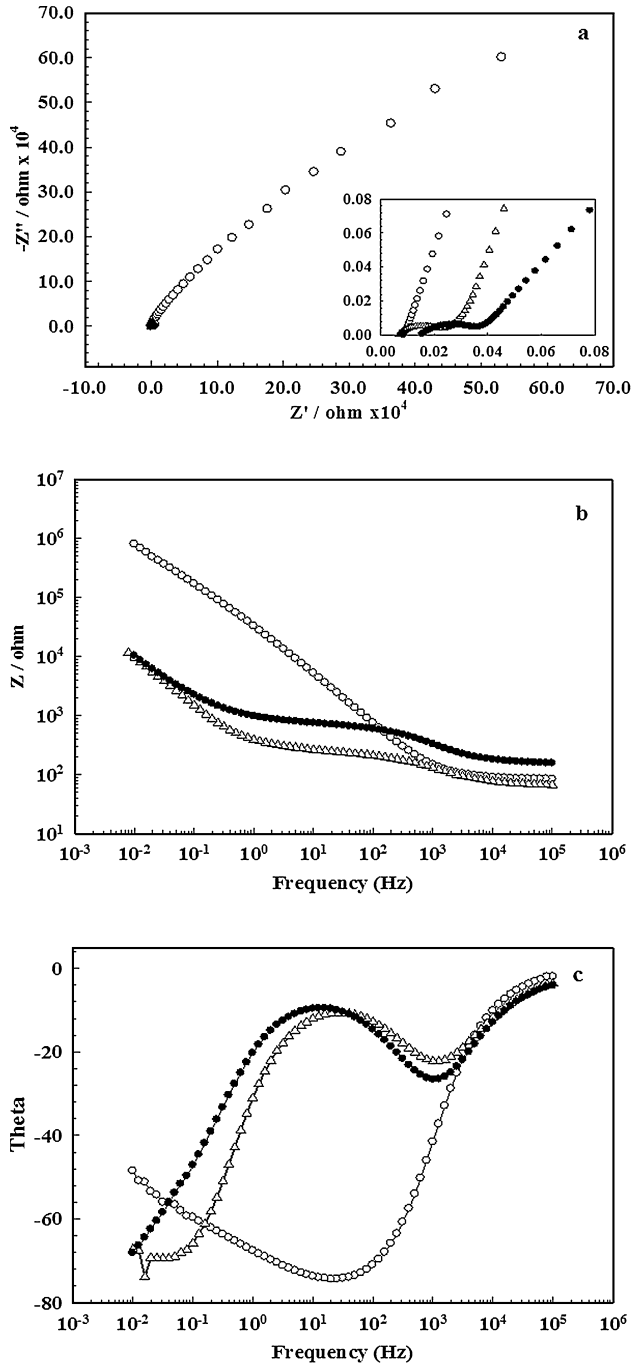

Fig. 4. Nyquist (a), Bode (b), phase angle-frequency (c) curves of SS (○), gel@Li (Δ) and gel@LiCu (●) electrodes at open circuit potantial under oxygen atmosphere in LED solution.

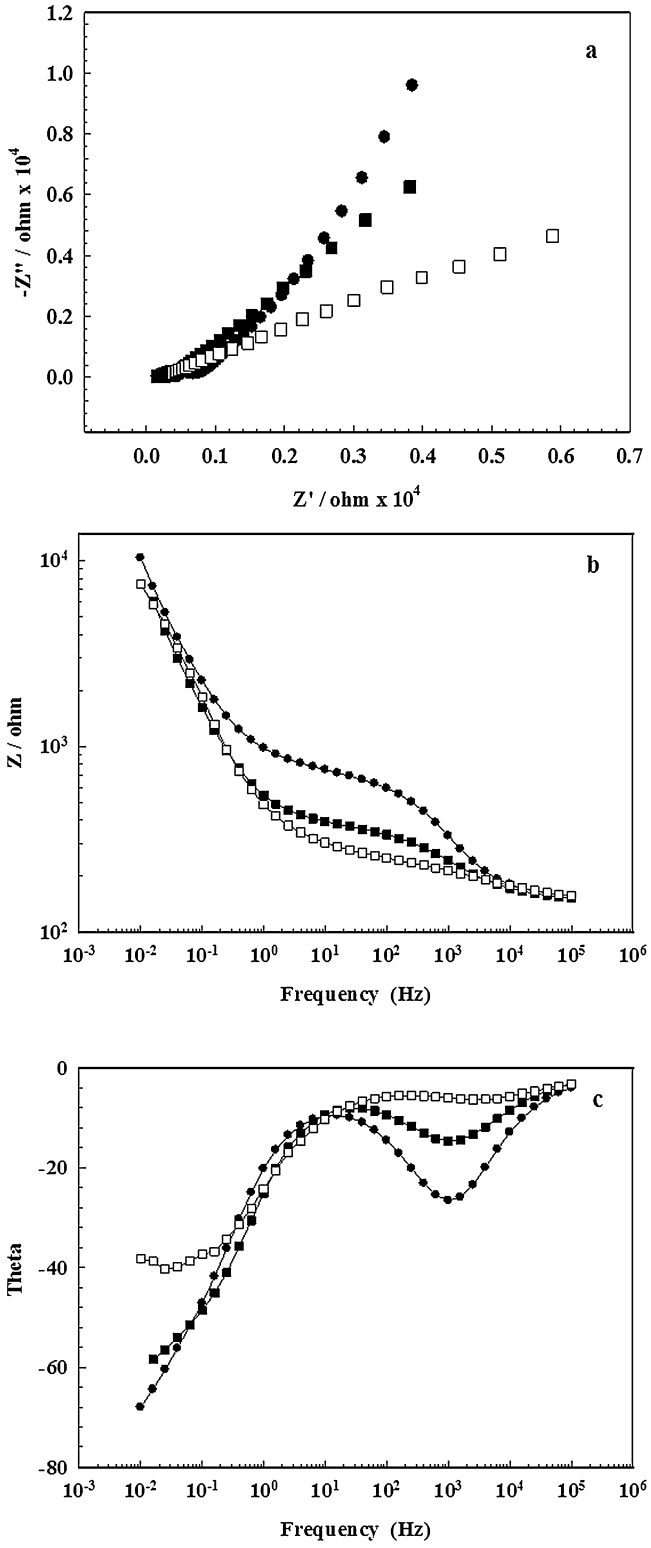

Fig. 5. Nyquist (a), Bode (b), phase angle-frequency (c) curves of gel@LiCu electrode at open circuit potantial (●), -1.7 V(□) and -1.0 V (■) in LED solution.

evolution reaction (OER) and oxygen reduction reaction (ORR) curves with Swagelok type test cell (MTI corporation). Surface characterization was made with X-ray diffraction (XRD, Rigaku, Rint-2000) using Cu Kα radiation and X-ray Fluorescence (XRF - PAM Analytical Advanced), using rhodium to check the chemical structures on the surface.

3. Results and discussion

Fig. 2 shows the cyclic voltammograms of electrodes, prepared from gel, gel + $LiNO_3$ (gel/Li), gel + $LiNO_3$ + $CuCl_2$ (gel/LiCu), activated carbon(@) supported gel + $LiNO_3$ (gel@Li) and activated carbon (@) supported gel + $LiNO_3$ + $CuCl_2$ (gel@LiCu) obtained in LED solution. Apparently, the current density of the gel electrode was lower than the current density of the gel/Li electrode. The current density increased as a result of addition of metal salts to the gel mixture. In lithium air batteries, the electrocatalytic effect of the cathode material can be enhanced by the addition of metal salts and metal oxides to the media [48]. In the voltammograms obtained with the gel@LiCu electrode the current density rose up to maximum. It has been proved that addition of carbon improves the electrical conductivity and performance of the materials [11]. The current density increases due to the widening of peaks and the alignment of peak potentials to positive and negative directions in the cathodic area.

During the gelling process, the efficiency of the electrodes, prepared with different amounts of glycine and various molar ratios of $LiNO_3$:$CuCl_2$ in the gel mixture, was determined. The best amounts of glycine and ratios of $LiNO_3$:$CuCl_2$ were selected as 0.2 g and 1.0:1.5, respectively. Hence, 0.2 g was preferred in the preparation of the gel mixture. The binding in the gel was weak when the glycine amount was more than 0.2 g. On the other hand, in gels with high glycine content, a sticky and adsorbate material was formed and the porosity was low on the electrode surface. Glycine and carboxylate groups are used together as coupling agents in the synthesis of nano particles and inorganic materials. In this case, glycine could be used both as a chelating agent, carbon source and a binder between chemicals in the gelling process [49].

In lithium air batteries, the contribution of binder, type of catalyst and carbon amount of the cathode material are important in preserving the electrode efficiency and preventing the blockage of its surface by Li_2O_2. The surface area and the catalytic properties of the cathode are significant for the electrochemical reactions in lithium air batteries. The wide surface area should be more electroactive for the convenient distribution of the catalyst particles. Furthermore, catalysts have large surface area and more active zones due to intercalating of lithium ions [50–52]. Therefore, the catalytic effect of the electrochemical reaction increases [8].

The current-potential curves were obtained in the oxygen-passing cell by using electrodes, which either include $CuCl_2$ (gel@LiCu) or don't (gel@Li). As seen in Fig. 3, the highest current density was procured with gel@LiCu electrode, while the lowest current density was observed with SS electrode. The current density obtained with the gel@LiCu electrode was higher than with other electrodes. The high current density shows that the prepared electrode is effective on the cathodic reaction in the working media. The open-circuit potentials of the SS, gel@Li and gel@LiCu electrodes were measured as -0.185 V, -0.146 V and -0.037 V respectively. Thus, the open-circuit potential of the gel@LiCu electrode tends to be more positive.

The Nyquist (a), Bode (b) and phase angle-frequency (c) curves that were obtained in the open-circuit potential of the SS, with gel@Li and gel@LiCu electrodes in the oxygen atmosphere are given in Fig. 4. As seen in Fig. 4 a, a single loop was formed in the high-frequency regions of the Nyquist curves while an angular part was formed in low frequency regions. Even though the single loop in the Nyquist curves disclose transfer resistance and diffuse layer resistance, the angular part shows that the event was diffusion controlled [53]. The Bode (b) and phase angle-frequency (c) curves support the Nyquist curves, which are seen in Fig. 4. The single loop observed in the high-frequency regions became smaller when $CuCl_2$ was added in the gel. In Fig. 4, the polarization resistance (R_p)

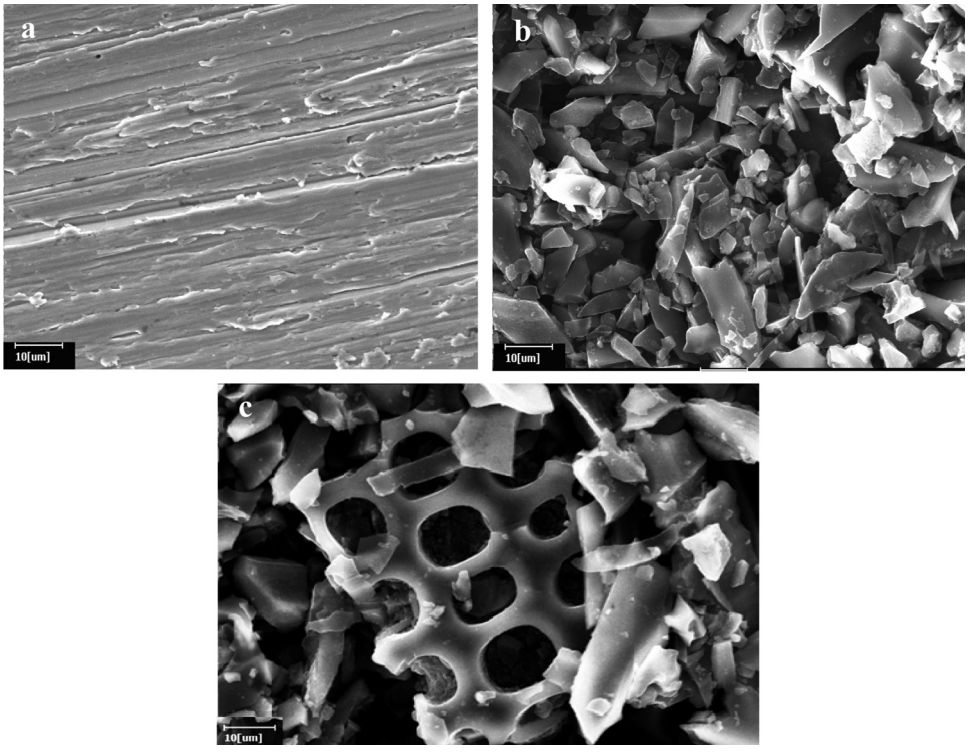

Fig. 6. SEM images of stainless steel (a), gel (b) and gel@LiCu (c) electrodes.

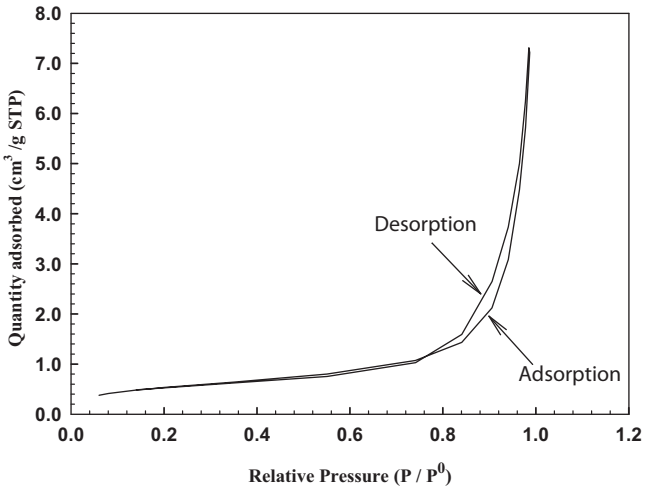

Fig. 7. N_2 adsorption-desorption isotherm of gel@LiCu catalyst.

value for gel@LiCu electrode is determined as 6.3 kΩ. The addition of $CuCl_2$ in the gel mixture increased the efficiency of the catalysts and decreased the polarization resistance.

Fig. 5, the Nyquist (a), Bode (b) and phase angle-frequency (c) curves obtained in LED solution under oxygen atmosphere by applying -1.7 V, -1.0 V and open circuit potentials to the gel@LiCu electrode. The polarization resistance decreases with applying the negative potential as seen in Fig. 5a. The obtained low resistances show that the electrochemical reaction proceeds efficiently on the surface at more negative potentials. The phase angle changes with potential at the frequency of 1.10^3Hz. This phenomenon could be related to the increasing of permeability and diffusion effect at more negative potentials [54].

The SEM images of all the electrodes are given in Fig. 6a and b. In Fig. 6a only emery traces are visible on the stainless steel surface. Fig. 6b shows that the gel prepared on stainless steel (kept for 4 days at 125 °C) is composed of close packed structures (one on the other) consisting of porous and small particles. In order to reach the efficient electrode performance, cathode active materials should have homogenous single phase, small particle size, porous structure and wide surface area [55–58].

The SEM image, which was obtained with the gel@LiCu catalyst is given in Fig. 6c. It can be observed that structure with a laminar layer was formed and, the surface was porous.

The N_2 adsorption–desorption isotherms for the gel@LiCu catalyst are shown in Fig. 7. Our sample fits to the type III, which gives adsorption isotherms on macroporous adsorbents with weak affinities [59]. The BET surface area, the total pore volume and the pore size for the gel@LiCu catalyst were 1.0886 $m^2 g^{-1}$ and 0.0105 $cm^3 g^{-1}$ and ~39 nm, respectively. The TEM images of the gel@LiCu catalyst are seen in Fig. 8. Fig. 8 a and b revealing presence of copper agglomerates and copper nanoparticles. The presence of copper in these catalysts provided high catalytic efficiency. These formations were supported by the N_2 adsorption isotherm and the SEM images. Pore size is an indicator for catalytic efficiency. The pore size of gel@LiCu catalyst, 39 nm, is bigger than the pore size of some studied catalysts, carbon aerogel pore size range 20–40 nm and it is about 10 times larger than the pore size of the activated carbon. According to the literature [60–62], the oxygen supply and electrolyte accessibility to the reaction site can be much easier through the pores of carbon aerogel.

As seen in Fig. 9, OER and ORR curves of gel@LiCu catalyst were determined at a current density of 0.1 mA cm^{-2}. On charge, positive overpotential is needed extra energy. On discharge, lithium peroxide increases the interval resistance of the cell and reduces reaction kinetics which is called negative overpotential. The voltage gap between the charging and discharging potentials is large because of dissociation of lithium peroxide. The use of a catalyst can decrease the overpotential and bring the potential closer to standart value[8]. The voltage gap (ΔV) between discharge and charge curves was 0.63 V as pointed out in Fig 9 for the gel@LiCu catalyst. In this case, oxygen evolution and reduction reactions were improved with Li-Cu bifunctional catalysts. The XRD data of our lithium-copper catalyst were analyzed in the range of $20° < 2\theta < 30°$ on an X-ray diffractometer (XRD Rigaku, Rint-2000) using CuKα radiation. The following reference numbers in the ICDD-PDF database were used for identification of crystalline phases: 4–836 (Cu), 5–667 (Cu_2O), 35–690 ($CuCl_2$), 25– 269 ($Cu_2(OH)_3Cl$) [63]. The diffraction peak was obtained at approximately $2\theta = 25°$ without any diffraction line concerned to crystalline forms. The X-ray diffraction spectrum of the gel@LiCu powders establishes the non-crystalline (amorphous) state of these materials [64]. XRD spectrum shows a broad peak at 25 θ . This means that the gel had an amorphous structure including copper and chloride. The copper content of the catalyst was analyzed by using X-ray Fluorescence (XRF). The XRF shows that the catalyst included (wt%): Cu:10.5817 ± 0.01; Cl:2.4148 ± 0.007; C:0.240 ± 0.001.

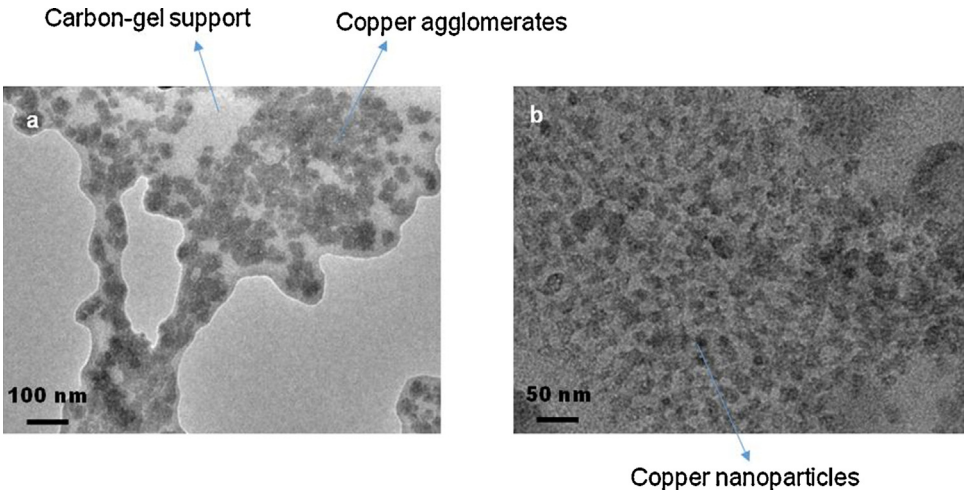

Fig. 8. TEM images of gel@LiCu catalyst (a) 200 nm and 500 nm (b).

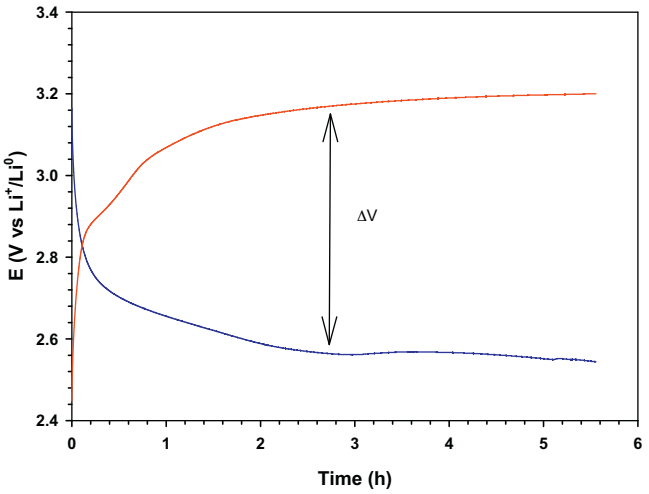

Fig. 9. OER and ORR curves of gel@LiCu catalyst at a current density of 0.1 mA cm^{-2}.

4. Conclusion

A mesoporous gel@LiCu catalyst was prepared and tested in oxygen reduction reaction for potential use as the cathode of lithium-air battery. The prepared catalyst efficiency was tested with cyclic voltammetry, EIS and discharge-charge curves. The composition and condition of the catalyst were optimized using cyclic voltammetry technique. The most suitable amount of glycine was determined as 0.2 g and the most efficient mol ratio of Li:Cu was selected as 1.0:1.5. The gel@LiCu catalyst exhibited low polarization resistance for efficient reduction of the oxygen on the surface. The SEM and TEM images show that the gel@LiCu electrode has a laminar and more porous structure. The porous form enhanced the catalytic efficiency of electrodes. This assumption was supported by cyclic voltammetry and EIS measurements. The results obtained from all the measurements proved that the gel@LiCu catalyst showed good efficiency towards oxygen reduction reaction and oxygen evolution reaction. It may be presumed that the prepared gel@LiCu could be used as a cathode catalyst for the lithium-air battery.

Acknowledgements

The authors are greatly thankful to Çukurova University Research Fund (Project Number:FEF2013D9) and The Scientific and Technological Research Council Of Turkey (TUBITAK) for financial support (Project Number: 112T532)

References

[1] P. Guan, G. Wang, C. Luo, K. Yan, E.J. Cairns, X. Hu, Comparisons of heat treatment on the electrochemical performance of different carbons for lithium-oxygen cells, Electrochim. Acta 129 (2014) 318–326.
[2] H. Minowa, M. Hayashi, K. Hayashi, R. Kobayashi, K. Takahashi, Mn-Fe-based oxide electrocatalysts for air electrodes of lithium-air batteries, J Power Sources 244 (2013) 17–22.
[3] K. Abraham, Z. Jiang, A Polymer Electrolyte-Based Rechargeable Lithium/Oxygen Battery, J. Electrochem. Soc. 143 (1996) 1–5.
[4] T. Ogasawara, A. Débart, M. Holzapfel, P. Novák, P.G. Bruce, Rechargeable Li2O2 electrode for lithium batteries, J. Am. Chem. Soc. 128 (2006) 1390–1393.
[5] Y. Wang, H. Zhou, A lithium-air battery with a potential to continuously reduce O2 from air for delivering energy, J. Power Sources 195 (2010) 358–361.
[6] J.S. Lee, S. Tai Kim, R. Cao, N.S. Choi, M. Liu, K.T. Lee, J. Cho, Metal–air batteries with high energy density: Li–air versus Zn–air, Advanced Energy Materials 1 (2011) 34–50.
[7] H. Cheng, K. Scott, Carbon-supported manganese oxide nanocatalysts for rechargeable lithium–air batteries, J. Power Sources 195 (2010) 1370–1374.
[8] R. Padbury, X. Zhang, Lithium–oxygen batteries—limiting factors that affect performance, J. Power Sources 196 (2011) 4436–4444.
[9] Y.G. Wang, H.S. Zhou, A new type rechargeable lithium battery based on a Cu-cathode, Electrochem Commun 11 (2009) 1834–1837.
[10] M. Armand, J.M. Tarascon, Building better batteries, Nature 451 (2008) 652–657.
[11] M.-K. Song, S. Park, F.M. Alamgir, J. Cho, M. Liu, Nanostructured electrodes for lithium-ion and lithium-air batteries: the latest developments, challenges, and perspectives, Materials Science and Engineering: R: Reports 72 (2011) 203–252.
[12] J. Read, Characterization of the lithium/oxygen organic electrolyte battery, J. Electrochem. Soc. 149 (2002) A1190–A1195.
[13] X.-h. Yang, P. He, Y.-y. Xia, Preparation of mesocellular carbon foam and its application for lithium/oxygen battery, Electrochem. Commun. 11 (2009) 1127–1130.
[14] S.S. Zhang, D. Foster, J. Read, Discharge characteristic of a non-aqueous electrolyte Li/O2 battery, J. Power Sources 195 (2010) 1235–1240.
[15] S. Monaco, A.M. Arangio, F. Soavi, M. Mastragostino, E. Paillard, S. Passerini, An electrochemical study of oxygen reduction in pyrrolidinium-based ionic liquids for lithium/oxygen batteries, Electrochim. Acta 83 (2012) 94–104.
[16] Y.C. Lu, Y. Shao-Horn, Probing the reaction kinetics of the charge reactions of nonaqueous Li-O2 batteries, Journal of Physical Chemistry Letters 4 (2013) 93–99.
[17] I. Landa-Medrano, I. Ruiz de Larramendi, N. Ortiz-Vitoriano, R. Pinedo, J. Ignacio Ruiz de Larramendi, T. Rojo, In situ monitoring of discharge/charge processes in Li–O2 batteries by electrochemical impedance spectroscopy, J. Power Sources 249 (2014) 110–117.
[18] Y.-C. Lu, Z. Xu, H.A. Gasteiger, S. Chen, K. Hamad-Schifferli, Y. Shao-Horn, Platinum-Gold Nanoparticles: A Highly Active Bifunctional Electrocatalyst for Rechargeable Lithium-Air Batteries, J. Am. Chem. Soc. 132 (2010) 12170–12171.
[19] Y.C. Lu, H.A. Gasteiger, Y. Shao-Horn, Catalytic activity trends of oxygen reduction reaction for nonaqueous Li-air batteries, J. Am. Chem. Soc. 133 (2011) 19048–19051.
[20] A. Concheso, R. Santamaría, M. Granda, R. Menéndez, J. Jiménez-Mateos, R. Alcántara, P. Lavela, J. Tirado, Influence of oxidative stabilization on the electrochemical behaviour of coal tar pitch derived carbons in lithium batteries, Electrochim. Acta 50 (2005) 1225–1232.
[21] F.-S. Ke, B.C. Solomon, S.-G. Ma, X.-D. Zhou, Metal–carbon nanocomposites as the oxygen electrode for rechargeable lithium–air batteries, Electrochim. Acta 85 (2012) 444–449.
[22] D.S. Kim, Y.J. Park, A simple method for surface modification of carbon by polydopamine coating for enhanced Li–air batteries, Electrochim. Acta 132 (2014) 297–306.
[23] W. Yang, J. Salim, S. Li, C. Sun, L. Chen, J.B. Goodenough, Y. Kim, Perovskite Sr0.95Ce0.05CoO3–δ loaded with copper nanoparticles as a bifunctional catalyst for lithium-air batteries, J. Mater. Chem. 22 (2012) 18902–18907.
[24] S.B. Ma, D.J. Lee, V. Roev, D. Im, S.G. Doo, Effect of porosity on electrochemical properties of carbon materials as cathode for lithium-oxygen battery, J Power Sources 244 (2013) 494–498.
[25] Z.H. Cui, X.X. Guo, Manganese monoxide nanoparticles adhered to mesoporous nitrogen-doped carbons for nonaqueous lithium–oxygen batteries, J. Power Sources 267 (2014) 20–25.
[26] Z. Guo, D. Zhou, X. Dong, Z. Qiu, Y. Wang, Y. Xia, Ordered Hierarchical Mesoporous/Macroporous Carbon: A High-Performance Catalyst for Rechargeable Li–O2 Batteries, Adv. Mater. 25 (2013) 5668–5672.
[27] H.-G. Jung, Y.S. Jeong, J.-B. Park, Y.-K. Sun, B. Scrosati, Y.J. Lee, Ruthenium-Based Electrocatalysts Supported on Reduced Graphene Oxide for Lithium-Air Batteries, ACS Nano 7 (2013) 3532–3539.
[28] J. Xiao, D. Mei, X. Li, W. Xu, D. Wang, G.L. Graff, W.D. Bennett, Z. Nie, L.V. Saraf, I. A. Aksay, J. Liu, J.-G. Zhang, Hierarchically Porous Graphene as a Lithium–Air Battery Electrode, Nano Lett. 11 (2011) 5071–5078.
[29] E. Yilmaz, C. Yogi, K. Yamanaka, T. Ohta, H.R. Byon, Promoting Formation of Noncrystalline Li2O2 in the Li–O2 Battery with RuO2 Nanoparticles, Nano Lett. 13 (2013) 4679–4684.
[30] R. Black, J.-H. Lee, B. Adams, C.A. Mims, L.F. Nazar, The Role of Catalysts and Peroxide Oxidation in Lithium–Oxygen Batteries, Angew. Chem. Int. Ed. 52 (2013) 392–396.
[31] Y. Yang, Q. Sun, Y.-S. Li, H. Li, Z.-W. Fu, A CoOx/carbon double-layer thin film air electrode for nonaqueous Li-air batteries, J. Power Sources 223 (2013) 312–318.
[32] F. Li, R. Ohnishi, Y. Yamada, J. Kubota, K. Domen, A. Yamada, H. Zhou, Carbon supported TiN nanoparticles: an efficient bifunctional catalyst for non-aqueous Li-O2 batteries, Chem. Commun. 49 (2013) 1175–1177.
[33] K. Zhang, L. Zhang, X. Chen, X. He, X. Wang, S. Dong, L. Gu, Z. Liu, C. Huang, G. Cui, Molybdenum Nitride/N-Doped Carbon Nanospheres for Lithium-O2 Battery Cathode Electrocatalyst, ACS Applied Materials & Interfaces 5 (2013) 3677–3682.
[34] K.-N. Jung, J.-I. Lee, W.B. Im, S. Yoon, K.-H. Shin, J.-W. Lee, Promoting Li2O2 oxidation by an La1.7Ca0.3Ni0.75Cu0.25O4 layered perovskite in lithium-oxygen batteries, Chem. Commun. 48 (2012) 9406–9408.
[35] J.-J. Xu, D. Xu, Z.-L. Wang, H.-G. Wang, L.-L. Zhang, X.-B. Zhang, Synthesis of Perovskite-Based Porous La0.75Sr0.25MnO3 Nanotubes as a Highly Efficient Electrocatalyst for Rechargeable Lithium–Oxygen Batteries, Angew. Chem. Int. Ed. 52 (2013) 3887–3890.
[36] S.H. Oh, R. Black, E. Pomerantseva, J.-H. Lee, L.F. Nazar, Synthesis of a metallic mesoporous pyrochlore as a catalyst for lithium–O2 batteries, Nat Chem 4 (2012) 1004–1010.

[37] S.H. Oh, L.F. Nazar, Oxide Catalysts for Rechargeable High-Capacity Li–O2 Batteries, Advanced Energy Materials 2 (2012) 903–910.
[38] Y.-C. Lu, Z. Xu, H.A. Gasteiger, S. Chen, K. Hamad-Schifferli, Y. Shao-Horn, Platinum- gold nanoparticles: A highly active bifunctional electrocatalyst for rechargeable lithium- air batteries, J. Am. Chem. Soc. 132 (2010) 12170–12171.
[39] W. Yang, J. Salim, C. Ma, Z. Ma, C. Sun, J. Li, L. Chen, Y. Kim, Flowerlike Co3O4 microspheres loaded with copper nanoparticle as an efficient bifunctional catalyst for lithium–air batteries, Electrochem. Commun. 28 (2013) 13–16.
[40] J.-K. Kim, W. Yang, J. Salim, C. Ma, C. Sun, J. Li, Y. Kim, Li-water battery with oxygen dissolved in water as a cathode, J. Electrochem. Soc. 161 (2014) A285–A289.
[41] X.Y. Cao, J.G. Xie, H. Zhan, Y.H. Zhou, Synthesis of CuV2O6 as a cathode material for rechargeable lithium batteries from V2O5 gel, Mater Chem Phys 98 (2006) 71–75.
[42] K.D. Kepler, J.T. Vaughey, M.M. Thackeray, Copper-tin anodes for rechargeable lithium batteries: an example of the matrix effect in an intermetallic system, J Power Sources 81 (1999) 383–387.
[43] C.-L. Li, Z.-W. Fu, Nano-sized copper tungstate thin films as positive electrodes for rechargeable Li batteries, Electrochim. Acta 53 (2008) 4293–4301.
[44] J. Morales, L. Sanchez, F. Martin, J.R. Ramos-Barrado, M. Sánchez, Nanostructured CuO thin film electrodes prepared by spray pyrolysis: a simple method for enhancing the electrochemical performance of CuO in lithium cells, Electrochim. Acta 49 (2004) 4589–4597.
[45] M. Hamdani, M. Pereira, J. Douch, A. Ait Addi, Y. Berghoute, M. Mendonça, Physicochemical and electrocatalytic properties of Li-Co3O4 anodes prepared by chemical spray pyrolysis for application in alkaline water electrolysis, Electrochim. Acta 49 (2004) 1555–1563.
[46] M. Hamdani, R. Singh, P. Chartier, Co3O4 and Co-based spinel oxides bifunctional oxygen electrodes, Int. J. Electrochem. Sci 5 (2010) 556–577.
[47] I. Nikolov, R. Darkaoui, E. Zhecheva, R. Stoyanova, N. Dimitrov, T. Vitanov, Electrocatalytic activity of spinel related cobalties MxCo3- xO4 (M= Li, Ni Cu) in the oxygen evolution reaction, J. Electroanal. Chem. 429 (1997) 157–168.
[48] S. Beattie, D. Manolescu, S. Blair, High-capacity lithium–air cathodes, J. Electrochem. Soc. 156 (2009) A44–A47.
[49] L. Wang, Z. Tang, L. Ma, X. Zhang, High-rate cathode based on Li3V2(PO4) 3/C composite material prepared via a glycine-assisted sol–gel method, Electrochem. Commun. 13 (2011) 1233–1235.
[50] J.J. Yu, J. Yang, W.B. Nie, Z.H. Li, E.H. Liu, G.T. Lei, Q.Z. Xiao, A porous vanadium pentoxide nanomaterial as cathode material for rechargeable lithium batteries, Electrochim. Acta 89 (2013) 292–299.
[51] F. Tu, T. Wu, S. Liu, G. Jin, C. Pan, Facile fabrication of MnO2 nanorod/graphene hybrid as cathode materials for lithium batteries, Electrochim. Acta 106 (2013) 406–410.
[52] C.-H. Ahn, R.S. Kalubarme, Y.-H. Kim, K.-N. Jung, K.-H. Shin, C.-J. Park, Graphene/doped ceria nano-blend for catalytic oxygen reduction in non-aqueous lithium-oxygen batteries, Electrochim. Acta 117 (2014) 18–25.
[53] G. Kardaş, B. Yazici, M. Erbil, Effect of some primary alcohols on hydrogen yield on platinum cathode in chloride solution, Int. J. Hydrogen Energy 28 (2003) 1213–1218.
[54] J.R. Scully, D.C. Silverman, M.W. Kendig, Electrochemical impedance: analysis and interpretation, ASTM International (1993) .
[55] J. Bates, N. Dudney, B. Neudecker, A. Ueda, C. Evans, Thin-film lithium and lithium-ion batteries, Solid State Ionics 135 (2000) 33–45.
[56] C.L. Campion, W. Li, W.B. Euler, B.L. Lucht, B. Ravdel, J.F. DiCarlo, R. Gitzendanner, K. Abraham, Suppression of toxic compounds produced in the decomposition of lithium-ion battery electrolytes, Electrochem. Solid-State Lett. 7 (2004) A194–A197.
[57] H. Chen, X. Qiu, W. Zhu, P. Hagenmuller, Synthesis and high rate properties of nanoparticled lithium cobalt oxides as the cathode material for lithium-ion battery, Electrochem. Commun. 4 (2002) 488–491.
[58] L.J. Hardwick, P.G. Bruce, The pursuit of rechargeable non-aqueous lithium–oxygen battery cathodes, Curr. Opin. Solid State Mater. Sci. 16 (2012) 178–185.
[59] M.D. Donohue, G.L. Aranovich, Classification of Gibbs adsorption isotherms, Adv Colloid Interfac 76 (1998) 137–152.
[60] Y. Gao, C. Wang, W. Pu, Z. Liu, C. Deng, P. Zhang, Z. Mao, Preparation of high-capacity air electrode for lithium-air batteries, Int. J. Hydrogen Energy 37 (2012) 12725–12730.
[61] S.B. Ma, D.J. Lee, V. Roev, D. Im, S.-G. Doo, Effect of porosity on electrochemical properties of carbon materials as cathode for lithium-oxygen battery, J. Power Sources 244 (2013) 494–498.
[62] M. Mirzaeian, P.J. Hall, Preparation of controlled porosity carbon aerogels for energy storage in rechargeable lithium oxygen batteries, Electrochim. Acta 54 (2009) 7444–7451.
[63] M. Chmielová, J. Seidlerová, Z. Weiss, X-ray diffraction phase analysis of crystalline copper corrosion products after treatment in different chloride solutions, Corros. Sci. 45 (2003) 883–889.
[64] Y. Idota, T. Kubota, A. Matsufuji, Y. Maekawa, T. Miyasaka, Tin-based amorphous oxide: a high-capacity lithium-ion-storage material, Science 276 (1997) 1395–1397.